ELSEVIER

Thermochimica Acta 377 (2001) 105–112

thermochimica acta

www.elsevier.com/locate/tca

Development of the front-detection photopyroelectric (FPPE) configuration for thermophysical study of glass-forming liquids

M. Chirtoc[a,1], E.H. Bentefour[a], C. Glorieux[a], J. Thoen[a,*]

[a]*Laboratorium voor Akoestiek en Thermische Fysica, Departement Natuurkunde, Katholieke Universiteit Leuven, Celestijnenlaan 200D, Leuven B-3001, Belgium*

Received 4 October 2000; received in revised form 27 February 2001; accepted 1 March 2001

Abstract

We report on the first frequency-dependent measurements of thermal effusivity of glass-forming liquids using the photopyroelectric (PPE) method. The advantage is higher modulation frequency capability than with previously reported methods. On the basis of our present results (up to 30 kHz), we find in the dispersion temperature region of glycerol a clear frequency-dependence of the real part and a non-zero, frequency-dependent imaginary part of the thermal effusivity, which is consistent with literature data. The experimental data reveal that the full exploitation of the high-frequency experimental results requires to take into account also the piezoelectric component of the signal caused by the thermoelastic response of the sample. The high-frequency limit of this PPE experiment may be extended by a modified cell design and by using another pyroelectric material instead of a lithium tantalate crystalline sensor.

Keywords: Photothermal; Photopyroelectric (PPE); Thermophysical properties; Thermal effusivity; Specific heat capacity; Glycerol

1. Introduction

The existence of a frequency-dependent specific heat near a glass transition is known since almost two decades but it is still a subject of theoretical and experimental investigations [1–3]. Studies reported in the literature have used dynamic calorimetric techniques [4] or the photoacoustic method [5–7] to determine almost exclusively the sample's thermal effusivity (a product of thermal conductivity and volume specific heat capacity). The methods were limited at high-frequency (some kHz) mainly by the size of the heaters that had to be very small (i.e. comparable to the thermal diffusion length at the highest frequency [3,8–10]), or by the transducer itself (microphone, etc. [5]).

The goal of this work is to investigate the temperature- and frequency-dependence of the thermophysical properties of a relatively thick sample in a wide frequency range. Pyroelectric sensors are ideally suited for this application which consists of ac temperature measurements by contact with the sample. Since the thermal excitation is provided by a laser beam, the method is called photopyroelectric (PPE) method

* Corresponding author. Tel.: +32-1632-7143; fax: +32-1632-7984.
E-mail address: jan.thoen@fys.kuleuven.ac.be (J. Thoen).
[1] On leave from the National Research and Development Institute for Isotopic and Molecular Technology, POB 700, 3400 Cluj-Napoca 5, Romania.

0040-6031/01/$ – see front matter
PII: S0040-6031(01)00545-7

[11]. Most PPE configurations rely on the propagation of heat waves across the sample (back-detection configuration, BPPE), or across the sensor (front-detection configuration with opaque electrodes, FPPE). Then the modulation frequency must be kept relatively low because thermal waves are strongly damped with propagation distance [12]. For high-frequency operation, a better configuration is one in which the heat source is located at (or very close to) the sensor–sample interface. This can be achieved with a thermally thick sensor and sample when at least one of them is transparent to the incident light. Therefore, we have adopted for our experimental cell a FPPE configuration with transparent front-electrode of the sensor [13].

2. Theory

The basic one-dimensional FPPE used throughout our experiments is represented schematically in Fig. 1. It consists of three adjacent layers: a pyroelectric sensor (p) in contact with infinitely thick sample material (m) and backing air (b). It is supposed that the backing and sensor materials are transparent, and that the sensor has a transparent electrode at the (b–p) interface and an opaque electrode at the (p–m) interface. The exciting radiation is incident from the backing-side and is absorbed at the (p–m) interface.

The FPPE configuration of Fig. 1 can be modeled theoretically by considering the corresponding particular case of the one-dimensional PPE theory with periodic excitation [14,15]. In general, the temperature (T) dependent PPE signal can be written as:

$$V(f,T) = V_0(T)\Gamma(f,T) \tag{1}$$

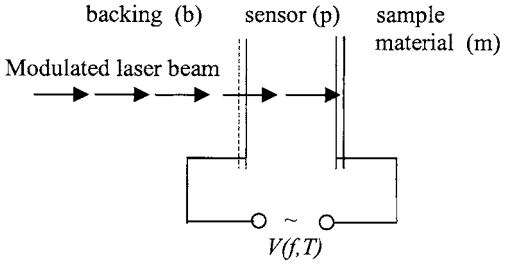

Fig. 1. One-dimensional configuration of the front-detection photopyroelectric (FPPE) cell with both, transparent backing material (b) and sensor (p). Optical absorption takes place at the (p–m) interface.

With a current preamplifier having a feed-back resistance R_f, the instrumental factor has the form:

$$V_0(T) = \frac{-p(T)H_0SR_f}{2L_pc_p(T)}$$

It contains mainly parameters related to the sensor; p and c_p are its pyroelectric coefficient and volume specific heat capacity, S and L_p the sensor's surface and thickness, while H_0 the modulated radiation flux. The factor $\Gamma(f,T)$ contains all sample-related parameters. In our experiments, the backing is air (negligible thermal effusivity), resulting in the following expression for $\Gamma(f,T)$:

$$\Gamma(f,T) = \frac{1}{1+b_{mp}}\frac{(1-e^{-2\sigma_pL_p})}{(1+R_{mp}e^{-2\sigma_pL_p})} \tag{2}$$

The notations are: $b_{mp} = e_m/e_p$ with $e = (ck)^{1/2}$ the thermal effusivity, c the volume specific heat capacity and k the thermal conductivity; $R_{mp} = (b_{mp}-1)/(b_{mp}+1)$ is the reflection coefficient of the thermal waves at the (m–p) interface, $\sigma = (1+i)/\mu$ the complex thermal diffusion coefficient with $\mu = (\alpha/\pi f)^{1/2}$ the thermal diffusion length and $\alpha = k/c$ the thermal diffusivity. In the low-frequency limit ($L_p/\mu_p \ll 1$) Eq. (2) can be approximated by $\Gamma(f,T) = (1+i)(\pi f)^{1/2}c_pL_p/e_m$ (signal phase = 45°), while in the high-frequency limit ($L_p/\mu_p \gg 1$) it becomes: $\Gamma(f,T) = (1+e_m/e_p)^{-1}$ (signal phase = 0°).

The sensitivities $S_{A,\varphi}$ of Eq. (2) to relative variations in $\mathrm{Re}(e_m)$ and in $\mathrm{Im}(e_m)$ can be defined as follows:

$$S_A(\mathrm{Re}(e_m)) = \frac{\Delta|\Gamma(f)|/|\Gamma(f)|}{\Delta\mathrm{Re}(e_m)/|e_m|} \tag{3}$$

$$S_\varphi(\mathrm{Im}(e_m)) = \frac{\Delta\varphi}{\Delta\mathrm{Im}(e_m)/|e_m|} \tag{4}$$

The phase sensitivity is expressed in radians. Values of $S_{A,\varphi} = \pm 1$ would mean a relation of direct or inverse proportionality between the respective quantities. With the realistic condition that $\mathrm{Im}(e_m) < \mathrm{Re}(e_m)$, the Eqs. (3) and (4) applied to Eq. (2) yield the same values. Numerical simulations with values of thermal parameters taken at 248 K are shown in Fig. 2. At low-frequency the sensitivities tend to -1, whereas at high-frequency one obtains:

$$S_A(\mathrm{Re}(e_m)) = S\varphi(\mathrm{Im}(e_m)) = -\frac{e_m}{e_m+e_p} = -0.205 \tag{5}$$

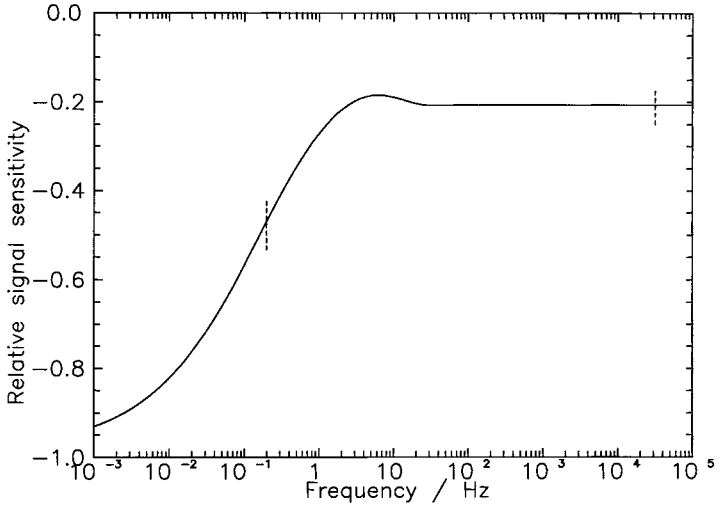

Fig. 2. Theoretical simulations of amplitude and phase sensitivities $S_A(\mathrm{Re}(e_\mathrm{m}))$ and $S_\varphi(\mathrm{Im}(e_\mathrm{m}))$ to changes in the complex thermal effusivity e_m of the sample, performed with Eqs. (2)–(4). The two curves are superposed. The experimental frequency range is indicated by the markers.

In practice this means that the influence of e_m on the high-frequency signal is reduced by a factor of $1/(-0.205) = -4.89$, depending on the effusivity ratio $e_\mathrm{m}/e_\mathrm{p}$. The high effusivity of lithium tantalate sensor used in conjunction with glycerol sample turns out to be rather unfavorable for the measurement of thermal effusivity in this configuration.

The cross-sensitivities $S_A(\mathrm{Im}(e_\mathrm{m}))$ and $S_\varphi(\mathrm{Re}(e_\mathrm{m}))$ are defined in a similar way to Eqs. (3) and (4). They have lower values than the previous ones and in the high-frequency limit they tend to zero. Therefore, at high-frequency, the signal amplitude depends only on $\mathrm{Re}(e_\mathrm{m})$ and the phase only on $\mathrm{Im}(e_\mathrm{m})$.

A variant of the FPPE configuration with opaque electrodes can be used to obtain a reference signal, V_ref, independent of the sample's properties. This is realized by irradiating the PPE cell from the right-hand side and by interchanging the (m) and (b) layers in Fig. 1. The optical absorption takes place now at the (p–b) interface. The signal response at high-frequency is obtained from Eq. (2) by replacing the subscript m by b:

$$\Gamma_\mathrm{ref}(f,T) = \frac{1}{1+b_\mathrm{bp}} \approx 1 \tag{6}$$

If (b) is air, $b_\mathrm{bp} = 1.7 \times 10^{-3} \ll 1$ and the signal is saturated, as if the sensor would be suspended in vacuum. Then from Eqs. (1) and (6), $V_\mathrm{ref}(f,T) = V_0(T)$ and it can be used as normalization signal for $V(f,T)$ to yield $\Gamma(f,T)$.

3. Experimental

The schematic cross-section of the experimental cell is shown in Fig. 3. The lateral wall consists of a glass cylinder joined to the upper and lower metallic lids by rubber O-rings. The cooling metal block is thermally insulated from the ambient with glass fiber foam. The air in the cell was kept dry during the measurements by placing inside a small quantity of silicagel crystals. For the pyroelectric sensor (a 15 mm × 15 mm × 0.3 mm $LiTaO_3$ crystal slab) it is essential to have a transparent ITO (indium tin oxide) upper electrode. The lower side and a part of the upper side were covered by vacuum deposited aluminum electrodes, in order to achieve opaque (p–m) and (b–p) interfaces necessary for the two measurement configurations. The frequency characteristics of the sensor alone proved that in both cases the electrodes were thermally thin beyond 30 kHz. The Pt temperature sensor was calibrated to an accuracy better than 0.1 K. The radiation source was a 20 mW HeNe laser, modulated by an acousto-optical modulator. The PPE signal was measured in current mode by a digital lock-in

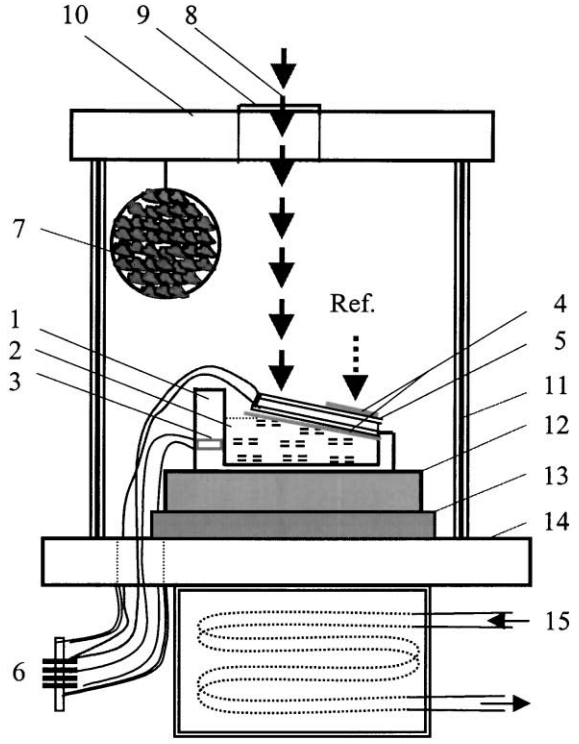

Fig. 3. Experimental FPPE cell and set up for measuring the temperature- and frequency-dependence of the thermophysical properties of glass-forming liquids. Two variants of the FPPE configuration are shown: opaque electrode at the sensor–sample interface, or at the air–sensor interface. The latter allows for the measurement of the reference signal. The components of the set up are: brass sample holder (1), liquid sample (2), temperature sensor with Pt resistance (3), aluminum electrodes (4), $LiTaO_3$ pyroelectric sensor with transparent electrodes (5), connections for PPE signal and for temperature sensor (6), silicagel crystals (7), modulated laser beam (8), glass window (9), metallic lid (10), glass wall (11), controlled heating stage (12), perspex plate (13), metallic support (14), inlet for liquid nitrogen vapors (15).

amplifier type Stanford SR 830. The set up was computer-controlled.

The temperature scans consisted in cooling the PPE cell down to 185 K during about 2 h. The data points were recorded every 0.1 K upon heating the cell back to room temperature with a heating rate of about 0.005 K/s. For the final results the data were averaged over 1 K. All measurements were repeated several times. Some measurements were performed also during cooling of the system, and no hysteresis phenomena were observed. This proves that no appreciable crystallization occurred during the thermal cycling of the sample.

The thermal parameters of $LiTaO_3$ are $e_p = 3575$ $Ws^{1/2}/m^2$ K and $\alpha_p = 1.367 \times 10^{-6}$ m^2/s at room temperature, and $e_p = 3425$ $Ws^{1/2}/m^2$ K and $\alpha_p = 1.577 \times 10^{-6}$ m^2/s at 248 K, by extrapolation of literature data [16]. Their temperature-dependence influences the results in several ways. First, the temperature-dependence of $V_0(T)$ (10% increase between 185 and 300 K, measured at 34 Hz) is eliminated by the normalization procedure, described earlier. Second, the factor $\Gamma(f,T)$ depends on $\alpha_p(T)$ and $e_p(T)$. We have taken into account these variations by the following fit polynomials:

$$\frac{e_p(T)}{e_p(-25^\circ C)} = 1.02432 + 9.730 \times 10^{-4} T(^\circ C) \quad (7)$$

$$\frac{\alpha_p(T)}{\alpha_p(-25^\circ C)} = 0.92605 - 2.9568 \times 10^{-3} T(^\circ C) \quad (8)$$

We have studied glycerol samples produced by Research Chemicals Ltd. with purity >99%. We used the following data for glycerol: $e_m = 933$ $Ws^{1/2}/m^2$ K and $\alpha_m = 9.45 \times 10^{-8}$ m^2/s at room temperature, and $e_m = 883$ $Ws^{1/2}/m^2$ K and $\alpha_m = 9.92 \times 10^{-8}$ m^2/s at 248 K, by extrapolation of product catalogue data from Kogyo Co., Japan.

For the inversion procedure we used an algorithm for minimization of complex quantities based on Eq. (2). Prior to this, the level of the normalized curves $V(f,T)/V_{ref}(f,T)$ was matched to the theoretical level of $\Gamma(f,T)$ at $T = 248$ K. This reference temperature is situated outside the dispersion region of glycerol, yet close enough to it in order to prevent errors due to systematic temperature drifts of experimental origin. In the determination of the complex quantity e_m^2 we have used the definition $e_m^2 = \mathrm{Re}(c_m k_m) - i\mathrm{Im}(c_m k_m)$ with a negative imaginary part according to the tradition in dielectric spectroscopy studies.

4. Results and discussion

The pyroelectric sensor used in this study has the thermally thin/thick limit $(L_p/\mu_p = 1)$ at 4.8 Hz. Below this frequency the signal amplitude is expected to decrease and the phase to increase, according to

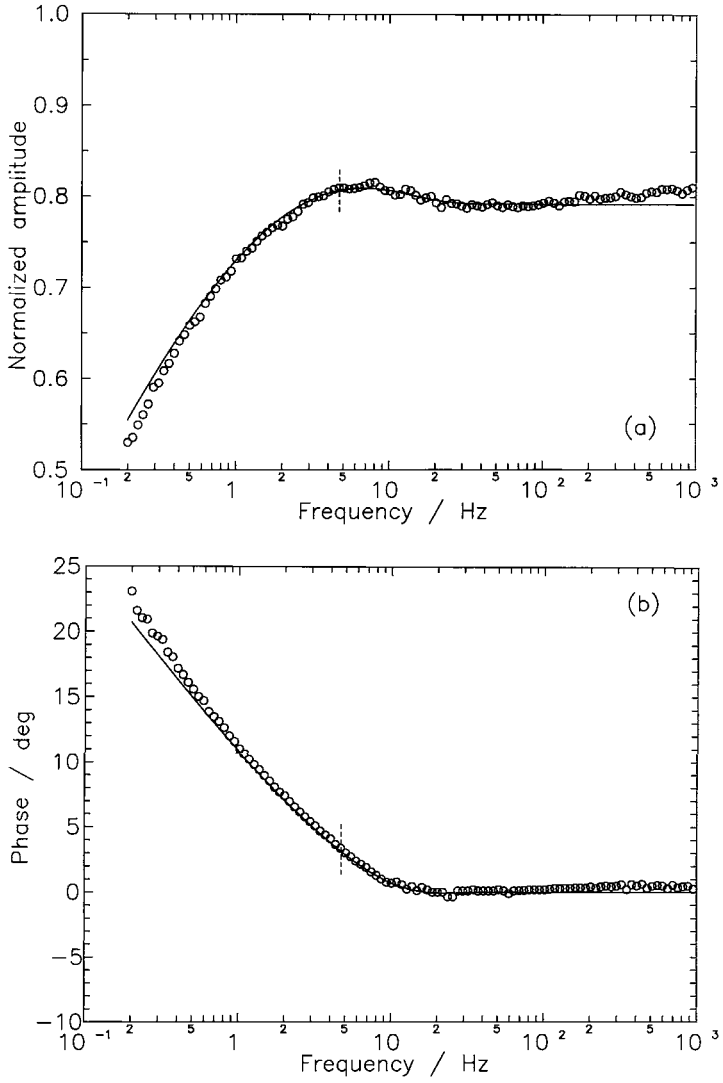

Fig. 4. Normalized amplitude (a) and phase (b) of PPE signal $\Gamma(f,T)$ at room temperature, as a function of frequency (circles). The theoretical curve based on Eq. (2) is also shown (solid line). The limit for the thermally thin/thick sensor at 4.8 Hz is indicated by the markers.

Eq. (2). The result of a frequency scan at room temperature (open circles) and the theoretical prediction (solid curves) are shown in Fig. 4. The small difference at very low-frequency is due to heat loss to the ambient air, not taken into account in the model. The agreement is however satisfactory, validating the theoretical approach.

Fig. 5 shows the temperature scans at the lowest and at the highest investigated frequencies, 0.2 Hz and 30 kHz. One can observe the temperature- and frequency-dependent features of glycerol, which are shifted from 194 K at 0.2 Hz to 229 K at 30 kHz. The theoretical sensitivities of Fig. 2 can explain the large difference between the relative variations at the two frequencies. At 0.2 Hz one has $S_A(\mathrm{Re}(e_\mathrm{m})) = S\varphi(\mathrm{Im}(e_\mathrm{m})) = -0.47$. Contrary to that, lower sensitivities (-0.205 from Eq. (8)) are expected at 30 kHz.

Fig. 6 shows the temperature-dependence of $\mathrm{Re}(c_\mathrm{m}k_\mathrm{m})$ and $\mathrm{Im}(c_\mathrm{m}k_\mathrm{m})$ of glycerol obtained from the curves $\Gamma(f,T)$ measured at different frequencies.

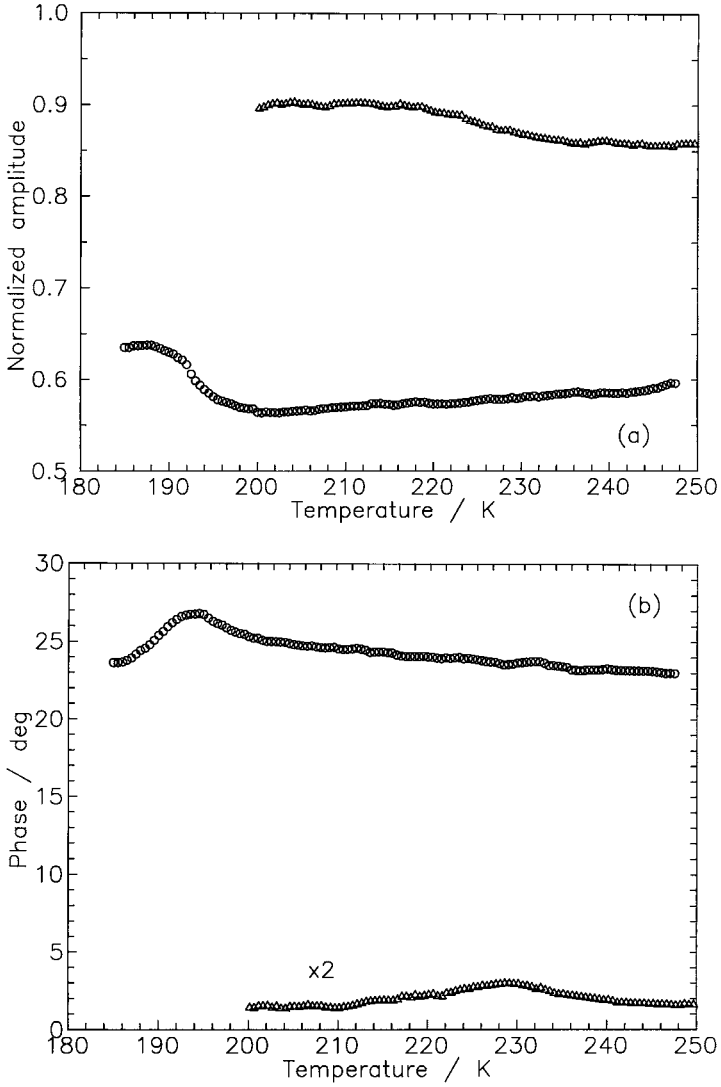

Fig. 5. Normalized amplitude (a) and phase (b) of PPE signals $\Gamma(f,T)$ at 0.2 Hz (○) and at 30 kHz (△) as a function of temperature. The dispersion regions (S-shaped amplitudes and peaked phases) are centered at 194 and 229 K, respectively.

First, the amplitudes and phases of $(c_m k_m)$ were determined. For each curve, the amplitude was normalized to unity at a temperature situated just above the respective dispersion region, and where the phase of $(c_m k_m)$ becomes 0. As a consequence, this condition normalizes both the real and imaginary parts of $(c_m k_m)$ shown in Fig. 6. In reality, the upper envelope of $\mathrm{Re}(c_m k_m)$ curves is not horizontal, due to a small decrease of the zero-frequency effusivity of glycerol with decreasing temperature. This would partially compensate for the increase at low temperature of the lower envelope of the $\mathrm{Re}(c_m k_m)$ curves. Another explanation of this increase might be the proximity of the glass transition.

In Fig. 6a, $\mathrm{Re}(c_m k_m)$ increases across the dispersion region by a factor 1.92 (factor 1.93 in [8]). The positions of the curves on the temperature axes in Fig. 6a and b are shifted by an average of 2 K towards

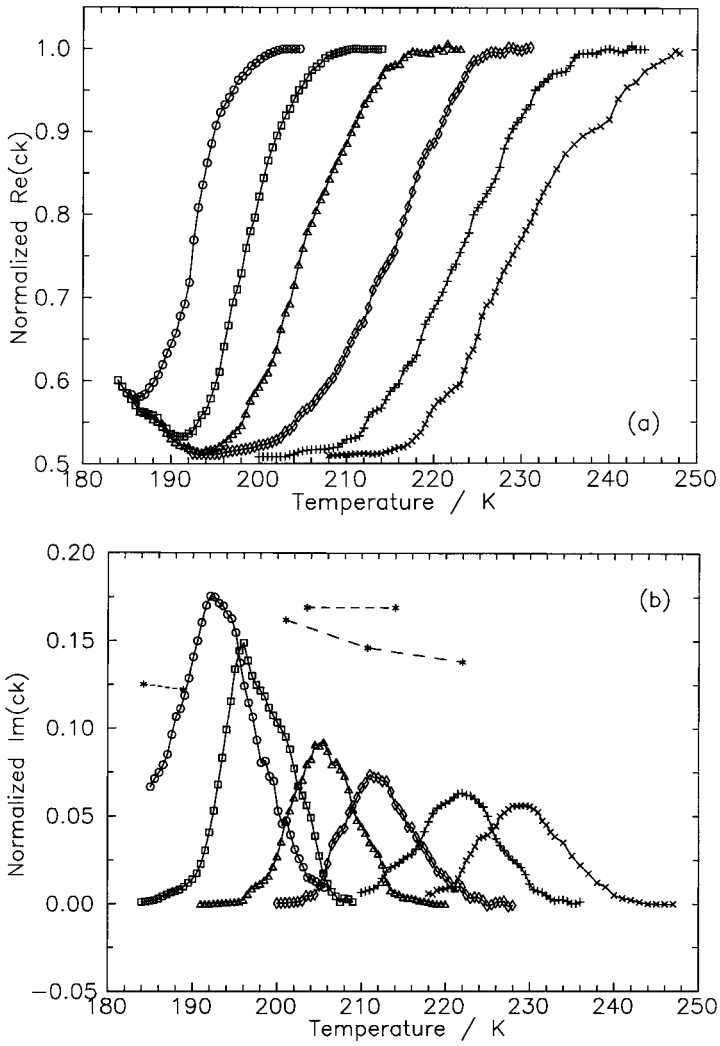

Fig. 6. The normalized quantities Re($c_m k_m$) (a) and Im($c_m k_m$) (b) as a function of temperature, at the following frequencies: 0.2 Hz (○), 2 Hz (□), 8 Hz (△), 120 Hz (◆), 3.5 kHz (+) and 30 kHz (×). For comparison, in (b) are also shown the positions of the top of the peaks (stars) from [8] (at 0.62, 34 and 1100 Hz, long dashes), from [7] (at 5 and 120 Hz, short dashes) and from [17] (2.4–35 mHz, dotted line).

lower temperatures in comparison to [8]. The peak heights of Im($c_m k_m$) (Fig. 6b) decrease at high-frequency, a feature that has been observed before [3,5,8], but not to such an extent. The symbols (stars) mark the positions of the top of the peaks as obtained in previous determinations [7,8,17]. At this stage we believe that the difference is due to the contribution of a thermoelastic component in our measured signal. The periodic thermal expansion of the sample in the region reached by the thermal wave is transformed into a piezoelectric signal by the lithium tantalate sensor, which is also piezoelectric. This contribution starts to become significant at high-frequency and affects in the first place the signal phase.

Another adverse effect we encountered was the amplitude instability with increasing frequency. The cause was probably the non-negligible contact thermal resistance between sample and sensor. In order to minimize this effect, one should decrease the sample quantity (and also the cell dimensions) thus reducing

the mechanical stress due to thermal expansion and contraction of the sample during the thermal cycles.

5. Conclusions

This work presents for the first time the application of the PPE method to the measurement of frequency-dependent thermophysical properties of glass-forming liquids. We demonstrate theoretically and experimentally that the PPE calorimetric method has the capability of high-frequency operation (up to 30 kHz in the present work), beyond the range of other existing techniques. Our present results confirm the known frequency-dependence of $\mathrm{Re}(c_m k_m)$ and $\mathrm{Im}(c_m k_m)$ in the dispersion region of glycerol.

The upper frequency limit found for the FPPE cell described in this work, is due to several causes: low sensitivity due to a substantial sample–sensor effusivity mismatch, the thermoelastic effect with the associated piezoelectric signal, and the sample–sensor thermal contact. All these drawbacks may be overcome by a modified design of the PPE cell and by the choice of another pyroelectric sensor material. They do not constitute intrinsic limitations for the application of the PPE method to the study of thermophysical properties of glass-forming liquids at high-frequency. Just recently, we have obtained good results for both the real and imaginary parts of the effusivity of glycerol up to 80 kHz, using a PVDF pyroelectric sensor [18]. Future work will be devoted to the use of different PPE configurations in order to determine directly other temperature- and frequency-dependent thermophysical properties.

Acknowledgements

One of the authors (M.C.) acknowledges the receipt of a fellowship granted by the Research Council of K.U. Leuven. This work was financially supported by the Fund for Scientific Research Flanders (Belgium) (Project No. G.0264.97).

References

[1] A.P. Sokolov, Science 273 (1996) 1675.
[2] J.K. Nielsen, J.C. Dyre, Phys. Rev. B 54 (1996) 15754.
[3] N. Menon, J. Chem. Phys. 105 (1996) 5246.
[4] N.O. Birge, S.R. Nagel, Rev. Sci. Instrum. 58 (1987) 1464.
[5] B. Büchner, P. Korpiun, Appl. Phys. B 43 (1987) 29.
[6] K.N. Madhusoodanan, K. Nandakumar, J. Philip, S.S.K. Titus, S. Asokan, E.S.R. Gopal, Phys. Stat. Sol. (a) 114 (1989) 525.
[7] S. Kojima, in: Proceedings of the IEEE Ultrasonics Symposium, Honolulu, HI, USA, 4–7 December 1990, Vol. 3, p. 1321.
[8] N.O. Birge, S.R. Nagel, Phys. Rev. Lett. 54 (1985) 2674.
[9] P.K. Dixon, S.R. Nagel, Phys. Rev. Lett. 61 (1988) 341.
[10] Y.H. Jeong, I.K. Moon, Phys. Rev. B 52 (1995) 6381.
[11] A. Mandelis, Chem. Phys. Lett. 108 (1984) 388.
[12] H. Coufal, A. Mandelis, Ferroelectrics 118 (1991) 379.
[13] M. Marinelli, F. Mercuri, U. Zammit, Appl. Phys. Lett. 65 (1994) 2663.
[14] A. Mandelis, M.M. Zver, J. Appl. Phys. 57 (1985) 4421.
[15] M. Chirtoc, G. Mihailescu, Phys. Rev. B 40 (1989) 9606.
[16] M. Marinelli, F. Murtas, M.G. Mecozzi, U. Zammitt, R. Pizzoferrato, F. Scudieri, S. Martellucci, M. Marinelli, Appl. Phys. A 51 (1990) 387.
[17] T. Christensen, Journal de Physique 46-C8 (1985) C8-635.
[18] E.H. Bentefour, M. Chirtoc, C. Glorieux, J. Thoen, Congrès Français de Thermique, SFT, Nantes, France, 29–31 May 2001, submitted for publication.